Hindawi
Journal of Nanomaterials
Volume 2022, Article ID 8946460, 19 pages
https://doi.org/10.1155/2022/8946460

Research Article

e-Modeling and Evolution of Nanolubricant Coupled Machining Parameters Using Statistical Tool

M. Sangeetha,[1] Lilly Mercy,[1] Dillipkumar Sahoo,[1] P. Gunasekar,[1] T. R. Praveenkumar ,[2] Habtamu Fekadu Gemede ,[3] and Rajesh Madasamy [2]

[1]*School of Mechanical Engineering, Sathyabama Institute of Science and Technology, India*
[2]*Department of Construction Technology and Management, Wollega University, P.O. Box 395, Nekemte, Ethiopia*
[3]*Department of Food Technology and Process Engineering, Wollega University, P.O. Box 395, Nekemte, Ethiopia*

Correspondence should be addressed to T. R. Praveenkumar; pravirami@gmail.com

Received 29 March 2022; Revised 28 April 2022; Accepted 5 May 2022; Published 13 June 2022

Academic Editor: V. Vijayan

Optimization is an essential action to select the effective input parameters for the responses obtained from machining. In this work, the combination of six sigma techniques and grey relational optimization are used for the corresponding input parameters, namely, spindle speed, feed rate, and drill diameter. The responses recorded are torque, thrust force, surface roughness, temperature, and ovality. Smaller the better response is preferred for all the output responses. Taguchi design of L27 array is preferred, and based on 27 combinations of input parameters, output responses are recorded. The thrust force and torque values are obtained in the graphical form during drilling process by the vertical machining center. After the drilling process the surface roughness of the hole is measured using profilometer. The probe in the profilometer is moved along the surface of the hole and the corresponding surface roughness values are noted for twenty-seven holes. The roundness of the hole is measured using a profile projector. The roundness of the hole is expanding due to the heat generated during the machining process. The expanded diameter of the hole is measured along the vertical and horizontal axes using the projector. Six sigma techniques are used to analyze the input parameters such as spindle speed, feed rate, and drill diameter. The optimization technique is used to determine the optimized parameters.

1. Introduction

Composites have the high specific strength and so the automobile and airplanes move at high speed with better fuel efficiency. Hybrid metal matrix composite is more advantageous compared to metal matrix composites since it is having the combined effect of improved mechanical properties, high wear resistance, and less wear of the tool while machining. Aluminium–Silicon-based metal matrix composites have major applications in automobile brakes and clutches. The orthogonal array, analysis of variance, and signal-to-noise ratio analyzed the machining parameters, and it also derived the optimal combination of input parameters. It is also proved that the Taguchi method derived the solution with minimum number of trials compared to the full factorial design [1]. Giasin and Ayvar-Soberanis measured the ovality error and burr height as the output responses in the drilling process. It was proved that the burr height at the exit is maximum than at the entry of the work piece. The ovality error and burr height is reduced at the minimum feed rate [2]. Fernandez-Perez et al. analyzed the output responses such as hole quality and tool wear. The influence of input parameters in drilling the output responses tool wear and hole quality was analyzed. The analytical study revealed that the input parameters, speed and feed, greatly influenced the output

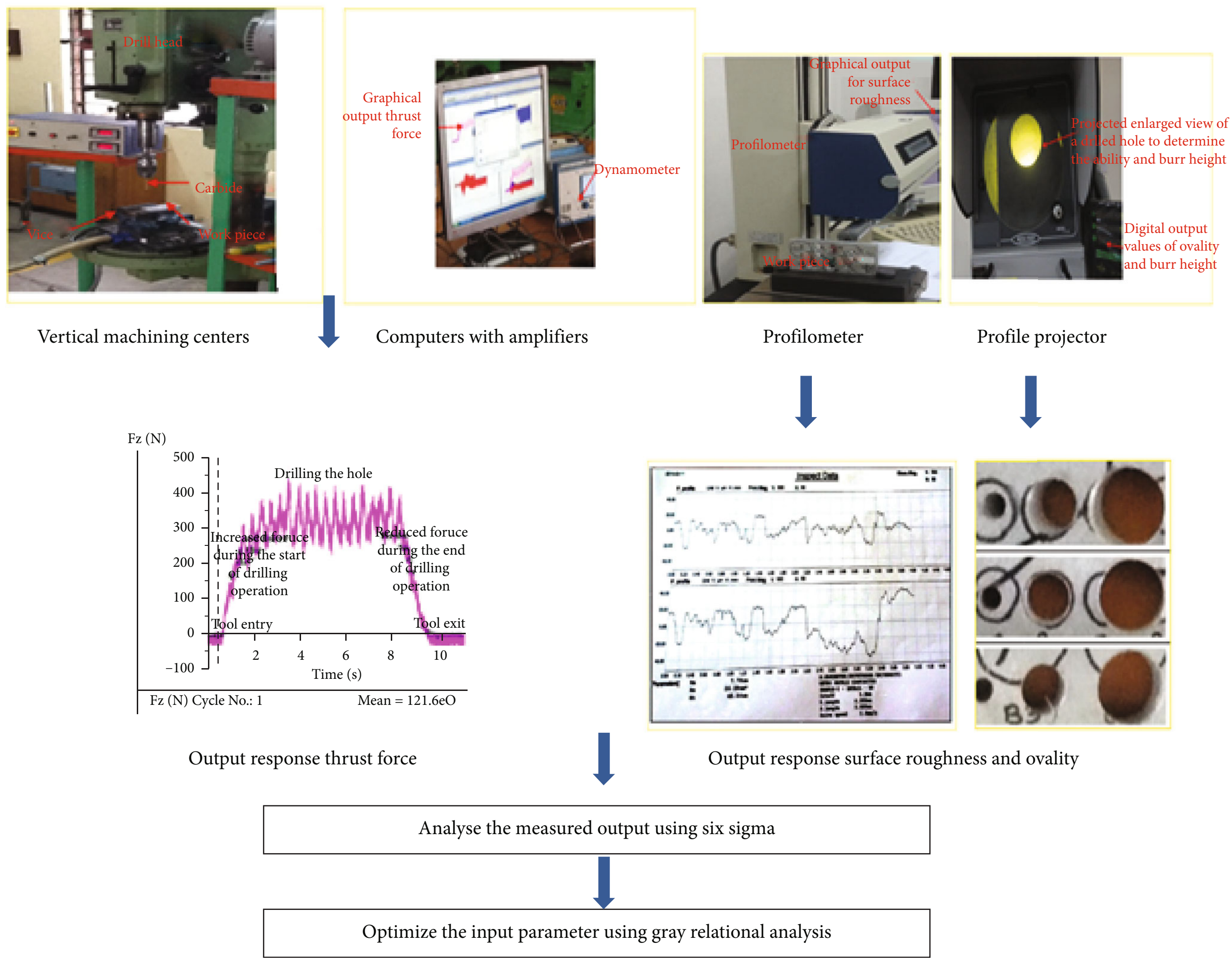

Figure 1: Experimental setup to record the output responses while drilling the metal matrix composites.

responses. The higher values of speed and feed resulted in less tool wear [3].

1.1. Literature on Machining of Metal Matrix Composites. Ekici et al. proved the reinforcement of solid lubricant graphite as a third element to the aluminum and boron carbide composites reduced the thrust force value to 25% compared to aluminum-boron carbide. The surface roughness value is greatly influenced by the percentage of graphite added with the aluminum-boron carbide composites [4]. The percentage of error between the predicted and validated values is 4.5 for the aluminum alloy reinforced with aluminum nitride so the optimization prediction is liable. The optimum condition for minimum surface roughness is uncoated carbide drills 320 m/min cutting speed, 0.4 mm/tooth feed rate, axial depth 0.4 mm, and 10% of reinforcement [5]. The optimal machining parameters while machining hybrid metal matrix composites LM 6/fly ash/silicon carbide particle is 175 m/min cutting speed, 0.25 mm depth of cut, and 0.1 mm/rev feed [6]. A review was made on machining hybrid metal matrix composites and concluded that the addition of third reinforcement with SiCp reduced the cutting force and improved the tool life and surface texture. In optimizing multiple responses, grey relational analysis is termed by the preferable technique by the researcher due to its simplicity [7]. Better hole quality and minimum surface roughness are achieved at maximum grey relational code value (GRC). The maximum value of GRC indicates the optimum input parameters and the maximum spindle speed; the minimum feed is termed as optimized values [8].

Priyadarshi and Sharma proved the reinforcement of nanosized silicon carbide particle in an aluminum alloy requires large cutting force (43 N) than hybrid reinforcement of nanosized silicon carbide particle and graphite requires less force (38 N). The optimization revealed that the hybrid reinforcement is better than individual reinforcement, and the confirmation test is within the acceptable limit of 5% [9]. The cutting speed influenced the surface roughness at the greater rate followed by feed and depth of cut. The error obtained is less than 5% between the modeled

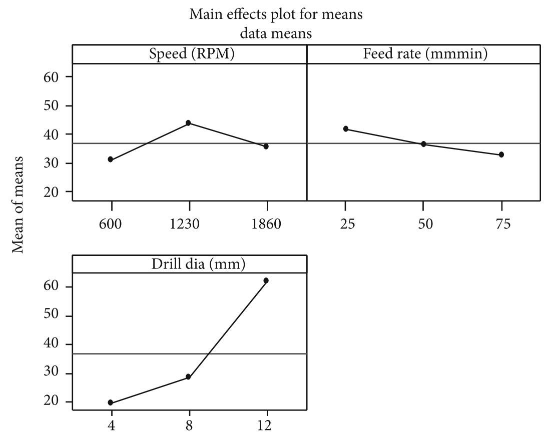

(a) Main effect plot for means

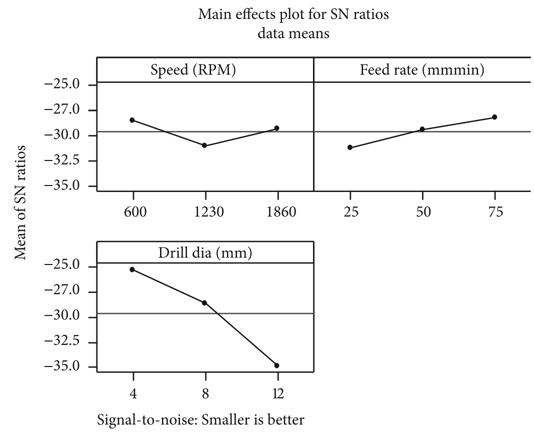

(b) Main effect plot for signal-to-noise ratio

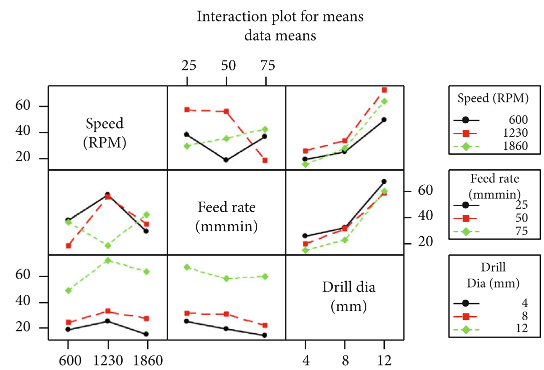

(c) Interaction plot for means

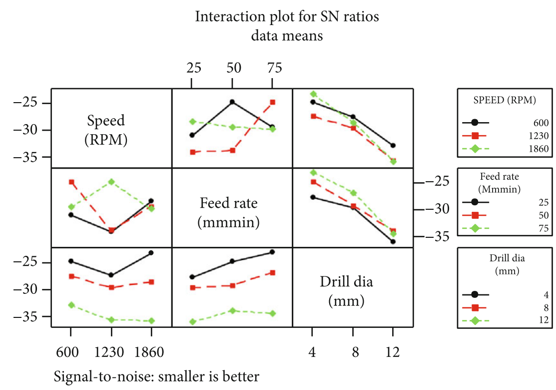

(d) Interaction plot for signal-to-noise ratio

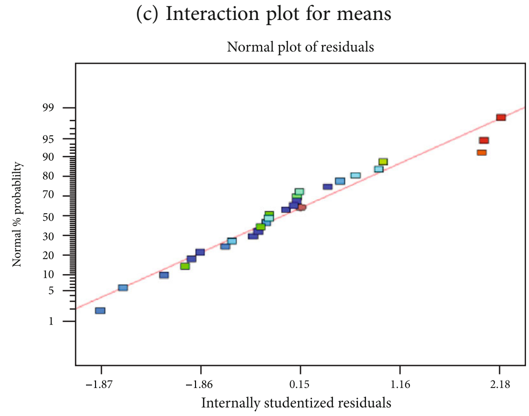

(e) Normal plot of residuals

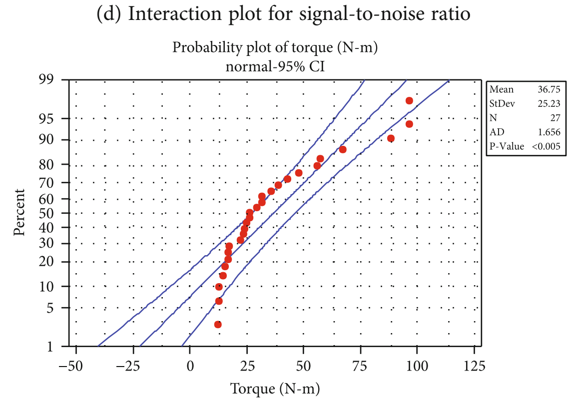

(f) Probability plot of torque

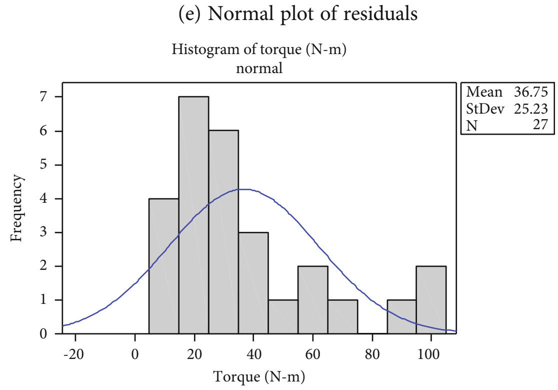

(g) Histogram of torque with respect to frequency

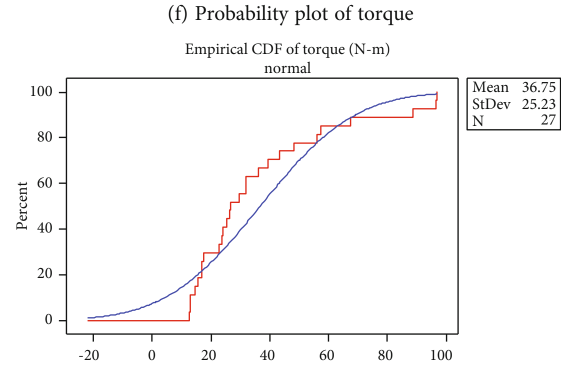

(h) Empirical CDF of torque

Figure 2: Continued.

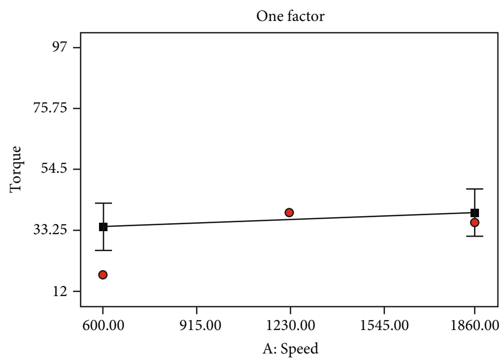

(i) Torque with respect to and feed

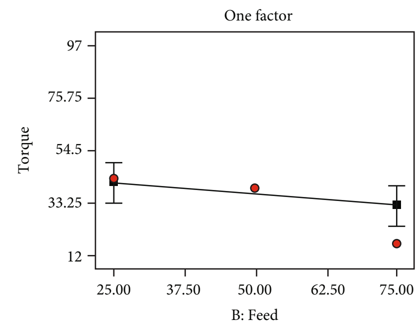

(j) Torque with respect to feed

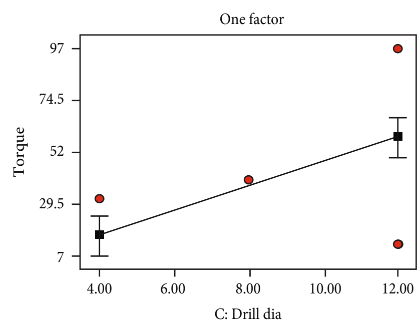

(k) Torque with respect to drill diameter

FIGURE 2: Analysis of torque using graphical output. R-square = 64.56% (obtained from response surface methodology).

TABLE 1: Response table for means (torque).

Level	Speed (rpm)	Feed rate (mm/min)	Drill diameter (mm)
1	30.82	41.49	19.61
2	43.87	36.34	28.42
3	35.55	32.42	62.21
Delta	13.05	9.07	42.59
Rank	2	3	1

TABLE 2: ANOVA table for torque.

Source	DF	Seq SS	Adj SS	Adj MS	F	P
Regression	9	10684.6	10684.6	1187.17	3.44	0.014
Linear	3	8635.3	837.8	279.25	0.81	0.506
Speed (rpm)	1	100.9	232.6	232.59	0.67	0.423
Feed (mm/min)	1	370.2	77.1	77.11	0.22	0.642
Drill diameter (mm)	1	8164.3	464.8	464.82	1.35	0.262
Square	3	1623.1	1623.1	541.05	1.7	0.234
Speed (rpm)*speed (rpm)	1	684.4	684.4	684.4	1.98	0.177
Feed rate (mm/min)* feed rate (mm/min)	1	2.3	2.3	2.28	0.01	0.936
Drill diameter (mm)* drill diameter (mm)	1	936.4	936.4	936.4	2.71	0.118
Interaction	3	426.1	426.1	142.02	0.41	0.747
Speed (rpm)* feed rate (mm/min)	1	161.7	161.7	161.7	0.47	0.503
Speed (rpm) * drill diameter (mm)	1	252.8	252.8	252.8	0.73	0.404
Drill diameter (mm) * feed rate (mm/min)	1	11.5	11.5	1.54	0.73	0.404
Residual error	17	5865.2	5862.2	345.01		
Total	26	16549.7				

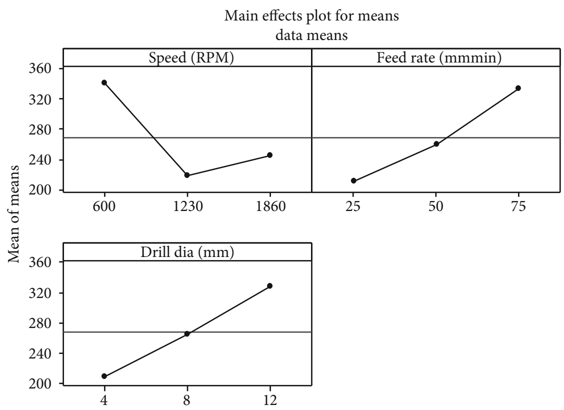

(a) Main effect plot for means

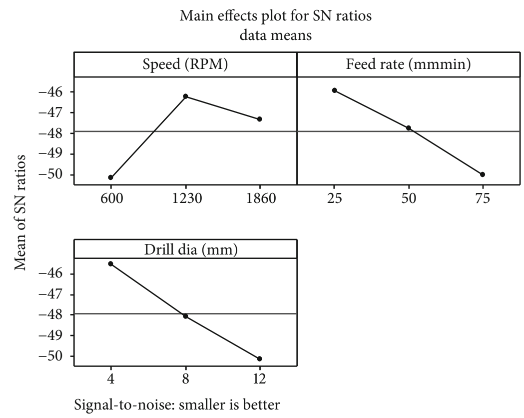

(b) Main effect plot for signal-to-noise ratio

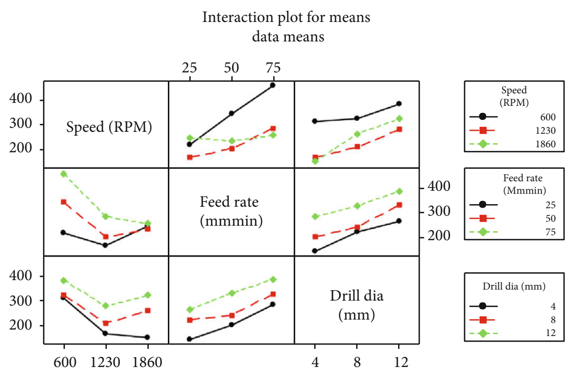

(c) Interaction plot for means

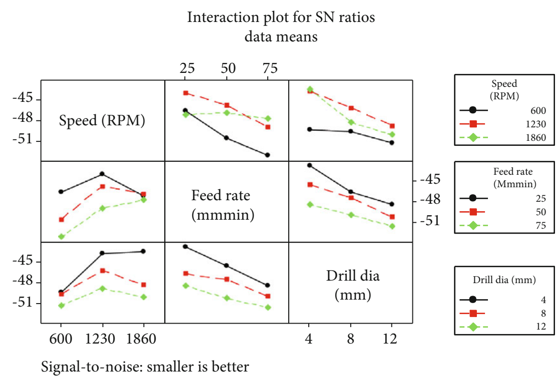

(d) Interaction plot for signal-to-noise ratio

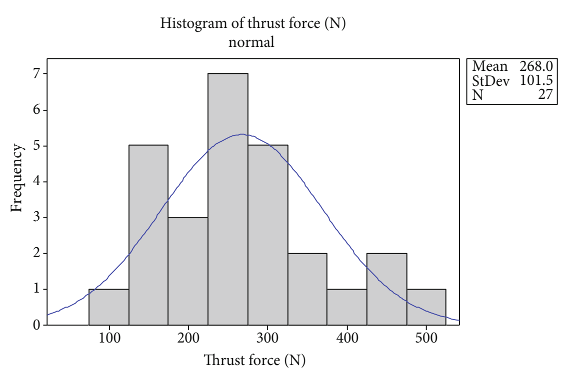

(e) Histogram of thrust force with respect to frequency

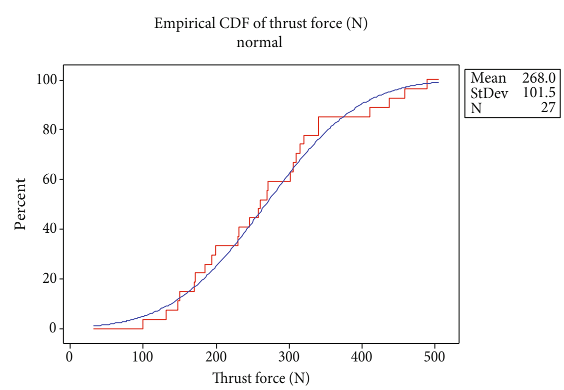

(f) Empirical CDF of thrust force

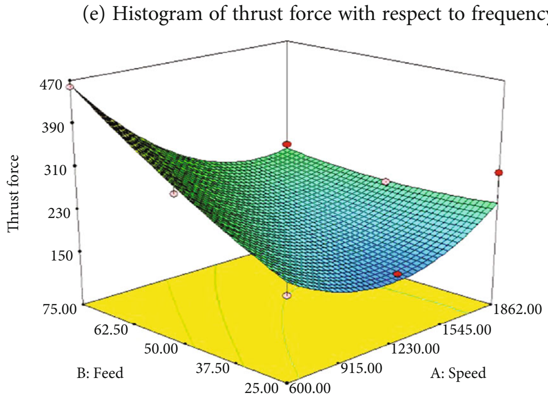

(g) 3D surface plot of thrust force with the combination of feed and speed

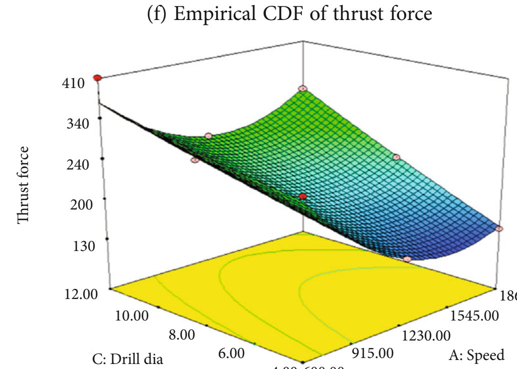

(h) 3D surface plot of thrust force with the combination of drill diameter and speed

FIGURE 3: Continued.

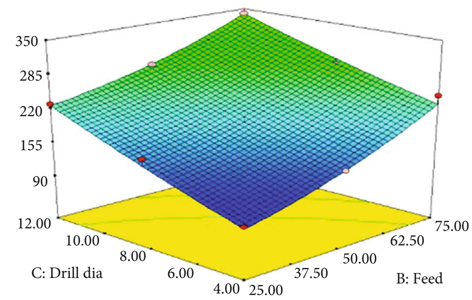

(i) 3D surface plot of thrust force with the combination of drill diameter and feed

Figure 3: Analysis of torque using graphical output. R-square = 96.78% (obtained from response surface methodology).

Table 3: Response table for means (thrust force).

Level	Speed (rpm)	Feed rate (mm/min)	Drill diameter (mm)
1	340.7	210.6	209.0
2	217.8	259.2	265.2
3	245.4	334.2	329.8
Delta	122.8	123.6	120.8
Rank	2	1	3

Table 4: ANOVA table for thrust force.

Source	DF	Seq SS	Adj SS	Adj MS	F	P
Regression	9	259359	259359	28817.6	56.86	0.001
Linear	3	175261	30792	10264.1	20.25	0.001
Speed (rpm)	1	40860	22955	22954.9	45.29	0.001
Feed (mm/min)	1	68734	5285	5284.9	10.43	0.005
Drill diameter (mm)	1	65667	8	7.8	0.02	0.903
Square	3	35084	35084	11694.7	23.08	0.001
Speed (rpm)*speed (rpm)	1	33930	33930	33930.2	66.95	0.001
Feed rate (mm/min)* feed rate (mm/min)	1	1048	1048	1048.1	2.07	0.169
Drill diameter (mm)* drill diameter (mm)	1	106	106	105.8	0.21	0.653
Interaction	3	49014	49014	16337.9	32.24	0.001
Speed (rpm)* feed rate (mm/min)	1	41290	41290	41289.6	81.47	0.001
Speed (rpm) * drill diameter (mm)	1	7420	7420	7420	14.64	0.001
Drill diameter (mm) * feed rate (mm/min)	1	304	304	304.0	0.60	0.449
Residual error	17	8616	8616	506.8		
Total	26	267974				

and experimental values [10]. Aluminum composites reinforced with silicon carbide particle with different mesh size reinforcements such as 220 and 600 using the machining process. The output response cutting force is greatly influenced by the feed and the depth of cut whereas surface roughness is influenced by feed and preheating temperature. Minimum cutting force is obtained at 80°C and 100°C, and a good surface finish is obtained at 60°C [11]. With the addition of the third element in metal matrix composites, it increased the wear and friction resistance. The optimum input parameters to obtain the minimum friction and wear are 15 N load and 3.25 m/sec sliding speed [12]. The grey relational code is maximum at 0.2 mm the depth of cut, 0.4 mm/rev feed, and 930 rpm speed. These optimal inputs reduced the surface roughness and tool temperature and maximize the material removal rate [13]. The material structure is the most significant factor for surface roughness, and the feed rate is the dominant factor that influences the thrust force in machining the aluminum alloy reinforced with alumina. The surface texture is increased by the addition of milled alumina with the aluminum alloy [14]. The optimized input parameters for better surface finish are cutting speed 900 rpm, feed rate 0.25 mm/rev, and depth of cut 0.5 mm. The feed has the major contribution of 82.6% followed by the depth of 6.8% and then cutting speed 6.43% [15]. The feed rate greatly influenced the thrust force and burr height

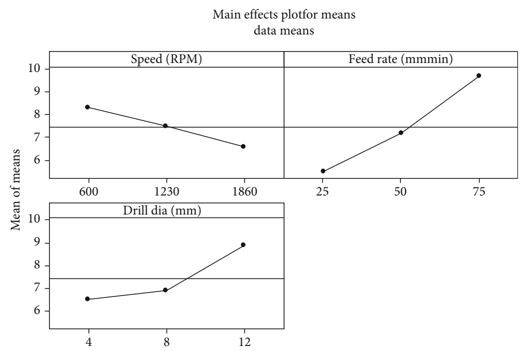

(a) Main effect plot for means

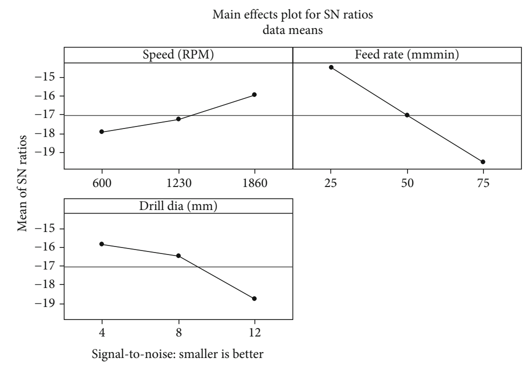

(b) Main effect plot for signal-to-noise ratio

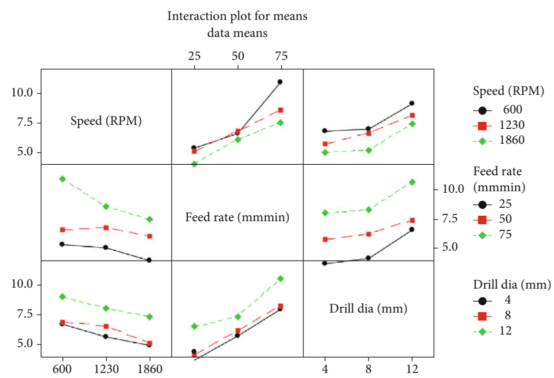

(c) Interaction plot for means

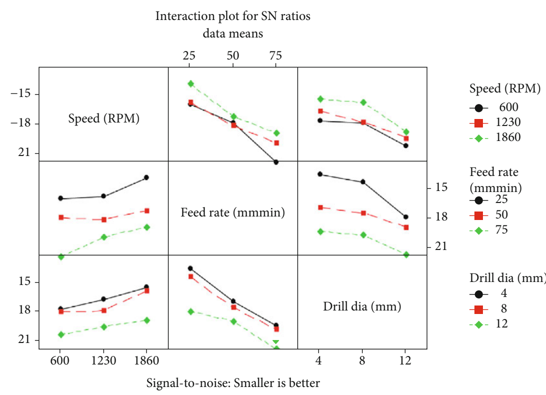

(d) Interaction plot for signal-to-noise ratio

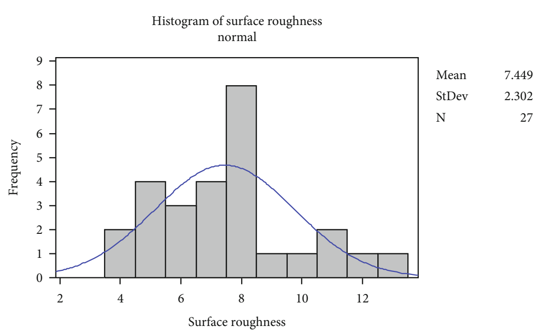

(e) Histogram of surface plot with respect to frequency

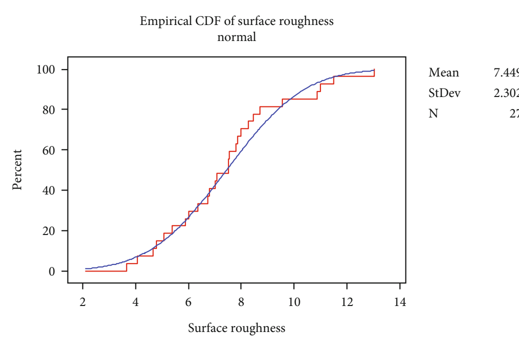

(f) Empirical CDF of surface roughness

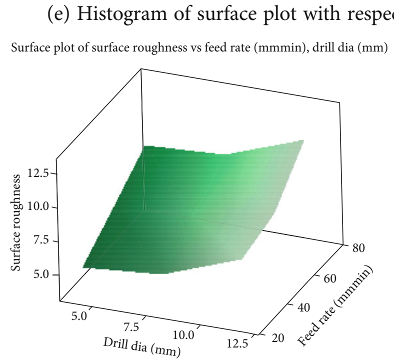

(g) 3D surface plot of surface roughness with respect drill diameter and feed rate

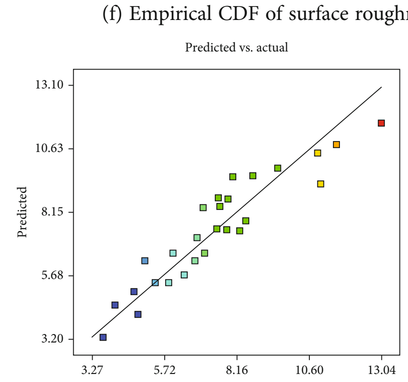

(h) Predicted value vs. actual value

Figure 4: Analysis of surface roughness using graphical output. R-square = 92.41% (obtained from response surface methodology).

Table 5: Response table for means (surface roughness).

Level	Speed (rpm)	Feed rate (mm/min)	Drill diameter (mm)
1	8.300	5.484	6.510
2	7.494	7.170	6.934
3	6.552	9.692	8.902
Delta	1.748	4.208	2.392
Rank	3	1	2

Table 6: ANOVA table for surface roughness.

Source (surface roughness)	DF	Seq SS	Adj SS	Adj MS	*F*	*P*
Regression	9	127.308	127.308	14.1453	22.98	0.001
Linear	3	119.173	2.020	0.6733	1.09	0.379
Speed (rpm)	1	13.746	0.044	0.0438	0.07	0.793
Feed (mm/min)	1	79.674	0.732	0.7324	1.19	0.291
Drill diameter (mm)	1	25.752	1.044	1.0443	1.70	0.210
Square	3	4.651	4.651	1.5503	2.52	0.093
Speed (rpm)* speed (rpm)	1	0.028	0.028	0.0280	0.05	0.834
Feed rate (mm/min)* feed rate (mm/min)	1	1.050	1.050	1.0500	1.71	0.210
Drill diameter (mm)* drill diameter (mm)	1	3.573	3.573	3.5728	5.81	0.028
Interaction	3	3.484	3.484	1.1615	1.89	0.170
Speed (rpm)* feed rate (mm/min)	1	3.435	3.435	3.4347	5.58	0.030
Speed (rpm) * drill diameter (mm)	1	0.022	0.022	0.217	0.04	0.853
Drill diameter (mm) * feed rate (mm/min)	1	0.028	0.028	0.05	0.834	
Residual error	17	10.463	10.463			
Total	26	137.771				

in drilling hybrid metal matrix composites (Al/15%SiC/4%graphite). The spindle speed is less influenced compared to the feed rate. At the lowest spindle speed of 1000 rpm and at a maximum feed rate of 1.5 mm/rev, the thrust force is 220 N [16].

Chaudhary et al. optimized aluminum silicate composite with spindle speed, feed rate, and drill diameter and output responses such as cylindricity, circularity, and surface finish, and various conclusions are made. The dimensional deviation is reduced with minimum drill bit diameter (6 mm). Circularity deviation is avoided at a minimum cutting speed (360 rpm) and minimum feed rate (0.095 mm/rev). Good surface finish is obtained by high cutting speed (680 rpm) and low feed rate (0.095 mm/rev). Cylindricity deviation is avoided with low spindle speed (680 rpm) and high feed rate (0.285 mm/rev) [17]. Confirmation test in optimizing A 356 reinforced with silicon carbide and boron carbide during machining operation revealed that the thrust force and surface roughness has 95% of the confidence interval. The analysis of variance deals with the influence of depth of cut and feed rate influence more with the cutting force and the surface roughness [18]. The best performance is obtained using uncoated carbide tool, the lower cutting speed of 119.2 m/min, and medium depth of cut 0.15 mm, and the corresponding grey relational grade value is 0.8084 [19]. The increased surface roughness (0.988 microns) is observed at high cutting speed (m/min) and high feed rate (mm/rev) at the higher percentage of reinforcement (15%) [20]. The feed greatly influenced the uncut fiber factor followed by drill diameter and spindle speed. The uncut fiber factor is reduced by increasing the drill diameter [21]. The addition of graphite in the mixture of aluminum and silicon carbide particle improved the machinability and increased the tribological properties. The confirmation test during optimization showed improvement from 0.619 to 0.891 percentage [22]. Ganesh and Chandrasekaran proved in their experiment that the thrust force values increased to a maximum of 200 N at a higher feed rate and at low speed of 500 rpm. When the speed rose to 1000 rpm, the thrust force decreased [23, 24].

The literature reviewed above explain the fabrication of composites and machining of the prepared specimen. It also includes the influence of input parameters with the output response using various analyzing tools. These research results in the greater influenced by feed and drill diameter on the output responses. In this paper, HMMCs (LM25/treated SiCp with MWCNT) are subjected to drilling process and the influence of input parameters are analyzed using mathematical modeling technique.

1.2. Scope and Objective. To perform the drilling operation on the specimen using the L_{27} orthogonal array. The drilling

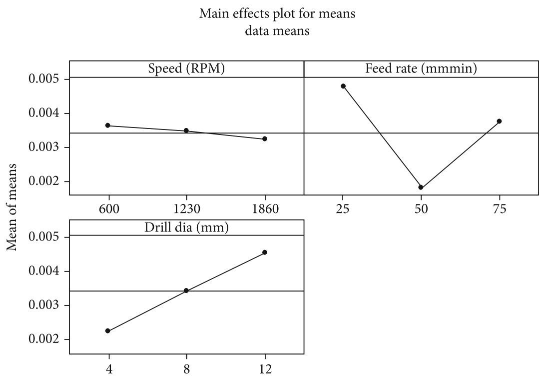

(a) Main effect plot for means

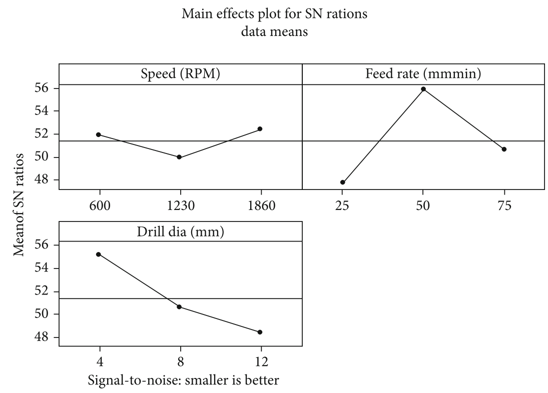

(b) Main effect plot for signal-to-noise ratio

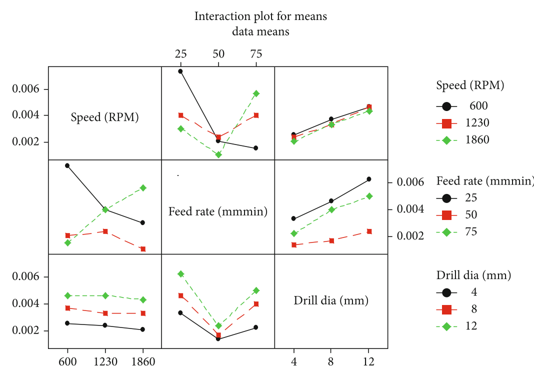

(c) Interaction plot for means

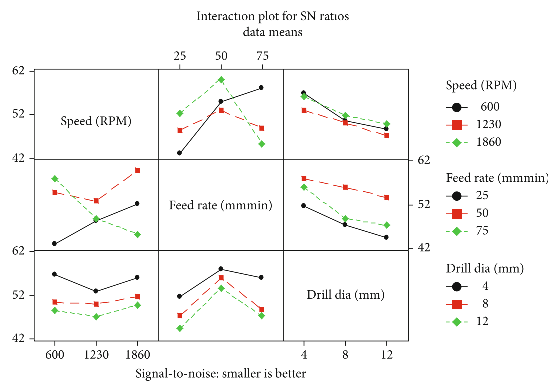

(d) Interaction plot for signal-to-noise ratio

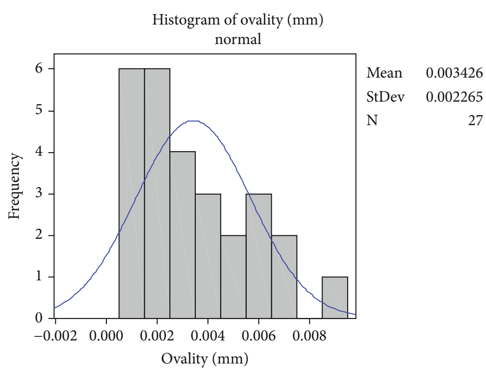

(e) Histogram of ovality with respect to frequency

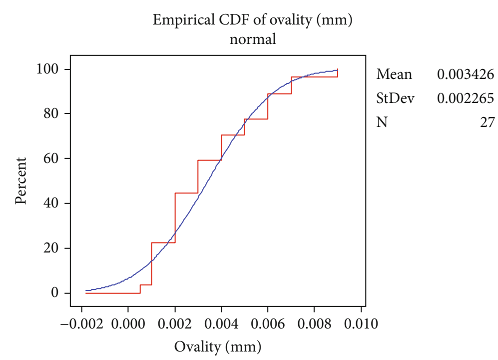

(f) Empirical CDF of ovality

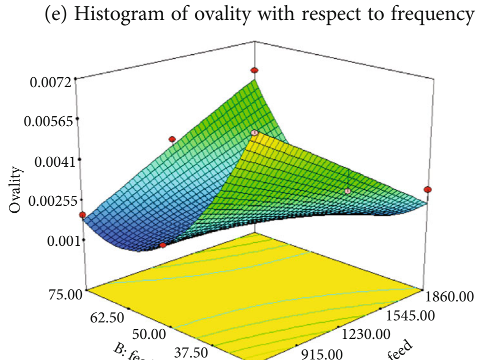

(g) 3D surface plot of ovality with respect to feed and speed

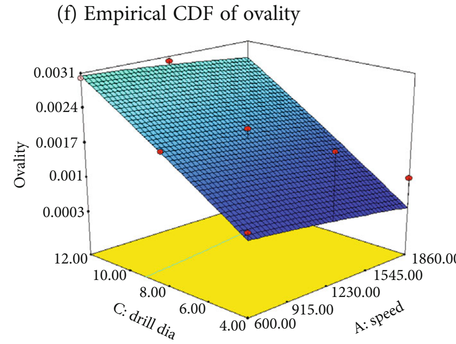

(h) 3D surface plot of ovality with respect to drill diameter and speed

Figure 5: Continued.

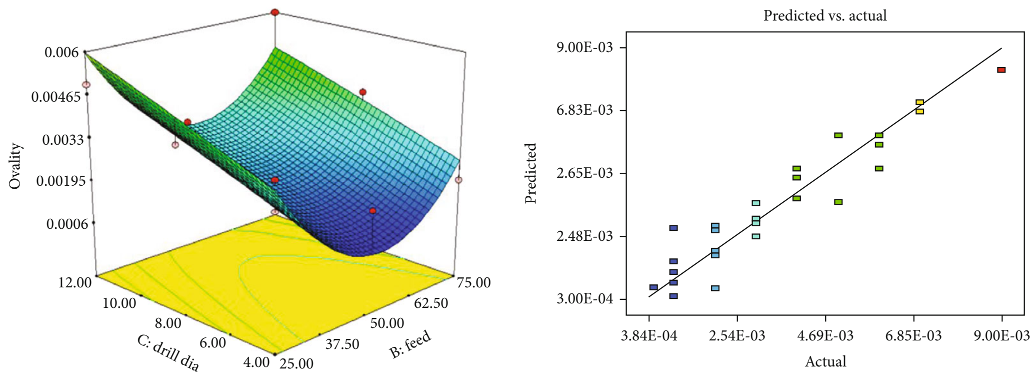

(i) 3D surface plot with respect to drill diameter and feed

(j) Predicted value vs. actual values

Figure 5: Analysis of ovality using graphical output. R-square = 89.95% (obtained from response surface methodology).

Table 7: Response table for means (ovality).

Level	Speed (rpm)	Feed rate (mm/min)	Drill diameter (mm)
1	0.003611	0.004778	0.002278
2	0.003444	0.001778	0.003444
3	0.003222	0.003722	0.004556
Delta	0.000389	0.003000	0.002278
Rank	3	1	2

Table 8: ANOVA table for ovality.

Source (ovality)	DF	Seq SS	Adj SS	Adj MS	F	P
Regression	9	0.000120	0.000120	0.000013	16.91	0.001
Linear	3	0.000029	0.000068	0.000023	28.6	0.001
Speed (rpm)	1	0.000001	0.000006	0.000006	7.59	0.014
Feed (mm/min)	1	0.000005	0.000062	0.000062	78.88	0.001
Drill diameter (mm)	1	0.000023	0.000	0.000	0.59	0.453
Square	3	0.000037	0.000037	0.000012	15.51	0.001
Speed (rpm)*speed (rpm)	1	0.000	0.000	0.000	0.01	0.940
Feed rate (mm/min)* feed rate (mm/min)	1	0.000037	0.000037	0.000037	46.52	0.001
Drill diameter (mm)* drill diameter (mm)	1	0.000	0.0000	0.0000	0.01	0.940
Interaction	3	0.000054	0.000054	0.000018	22.93	0.001
Speed (rpm)* feed rate (mm/min)	1	0.000054	0.000054	0.000054	68.74	0.001
Speed (rpm) * drill diameter (mm)	1	0.000	0.000	0.000	0.03	0.873
Drill diameter (mm) * feed rate (mm/min)	1	0.000	0.000	0.000	0.03	0.873
Residual error	17	0.000013	0.000013	0.000001		
Total	26	0.000133				

operation is done by considering the spindle speed, feed rate, and drill diameter as input parameter, and the output responses observed are thrust force, surface roughness, and ovality, to conduct wear test using the pin on disc device with inputs load, velocity, and percentage of reinforcement, to analyze the outputs responses using the statistical tool, and to optimize the input parameters using grey relational grade (GRG).

1.3. Methodology. The drilling process performed in the product with improved mechanical properties. The input parameters in drilling process are spindle speed, feed rate, and drill diameters of three different ranges, and the output responses recorded during machining process are torque, thrust force, surface roughness, ovality, and temperature. The effect of input parameters on the output responses is analyzed using response surface methodology and six sigma

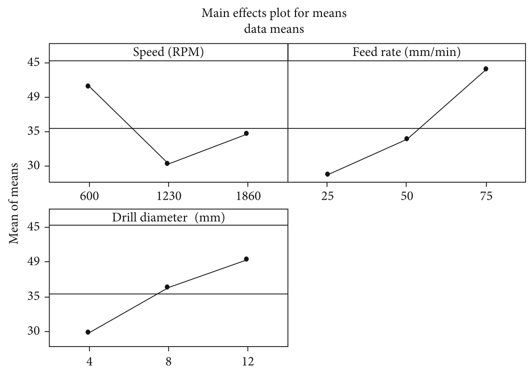

(a) Main effect plot for means

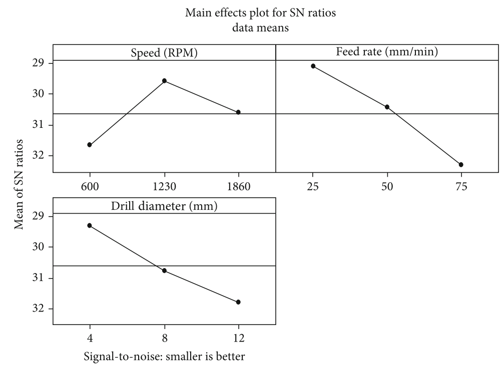

(b) Main effect plot for signal-to-noise ratio

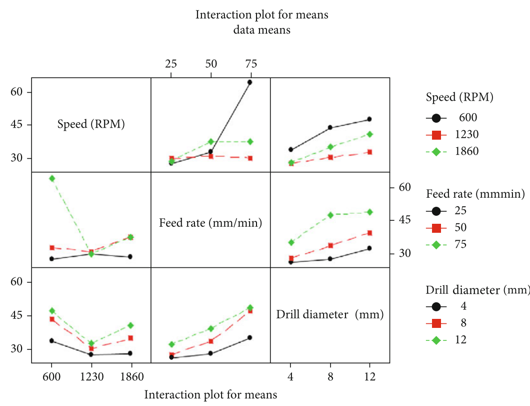

(c) Interaction plot for means

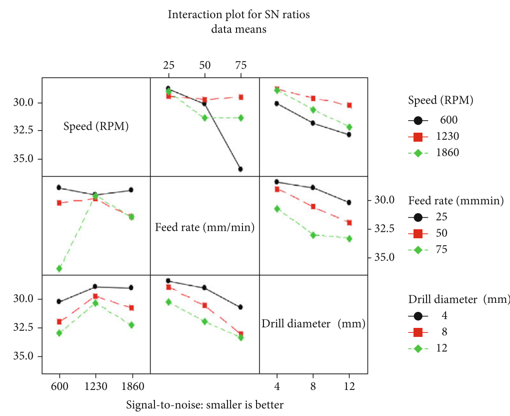

(d) Interaction plot for signal-to-noise ratio

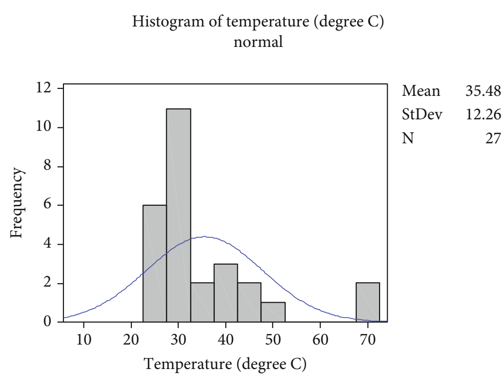

(e) Histogram of temperature with respect to frequency

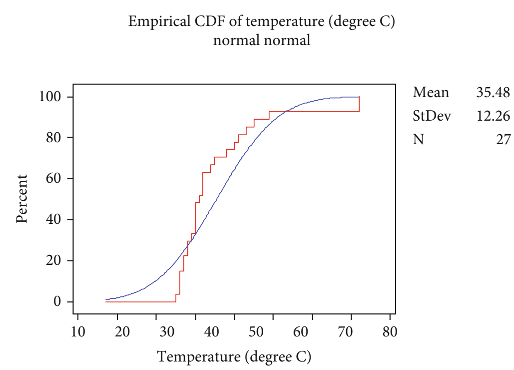

(f) Empirical CDF of temperature

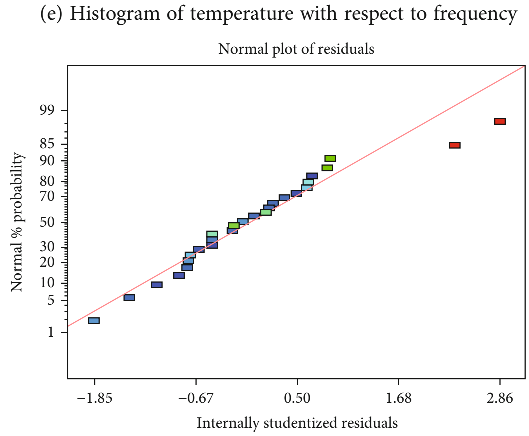

(g) Normal plot of residuals

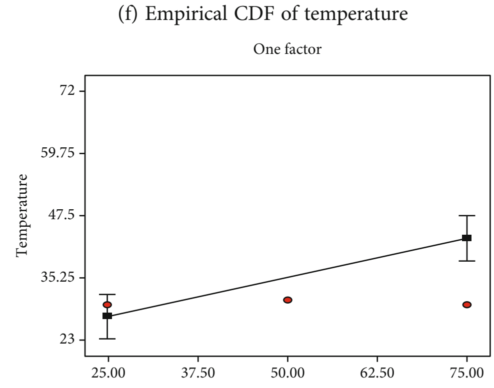

(h) Temperature plot with respect to speed

Figure 6: Continued.

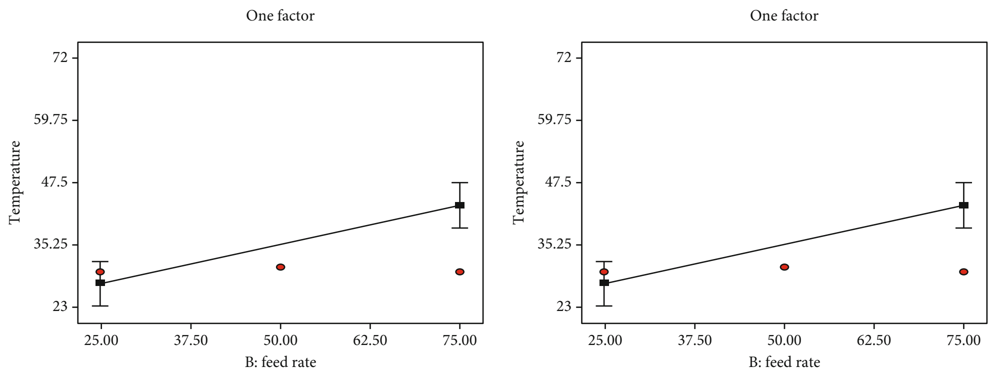

(i) Temperature plot with respect to feed rate (j) Temperature plot with respect to drill diameter

Figure 6: Analysis of temperature using graphical output. $R-\text{square}=71.86\%$.

Table 9

(a) Response table for means (temperature)

Level	Speed (rpm)	Feed rate (mm/min)	Drill diameter (mm)
1	41.56	28.67	29.78
2	30.22	33.78	36.33
3	34.67	44	40.33
Delta	11.33	15.33	10.56
Rank	2	1	3

(b) ANOVA table for temperature

Source (temp)	DF	Seq SS	Adj SS	Adj MS	F	P
Regression	9	2810.08	2810.08	312.231	4.82	0.003
Linear	3	1772.94	169.74	56.580	0.87	0.474
Speed (rpm)	1	213.56	123.58	123.578	1.91	0.185
Feed (mm/min)	1	1058.00	15.72	15.719	0.24	0.629
Drill diameter (mm)	1	501.39	14.72	14.725	0.23	0.640
Square	3	422.39	422.39	140.796	2.17	0.128
Speed (rpm)*speed (rpm)	1	373.40	373.41	373.407	5.77	0.028
Feed rate (mm/min)* feed rate (mm/min)	1	39.19	39.19	39.185	0.61	0.447
Drill diameter (mm)* drill diameter (mm)	1	9.80	9.80	9.796	0.15	0.702
Interaction	3	614.75	614.75	204.917	3.17	0.051
Speed (rpm)* feed rate (mm/min)	1	574.08	574.08	574.083	8.87	0.008
Speed (rpm) * drill diameter (mm)	1	0.33	0.33	0.333	0.01	0.944
Drill diameter (mm) * feed rate (mm/min)	1	40.33	40.33	40.333	0.62	0.441
Residual error	17	1100.66	1100.66	64.745		
Total	26	3910.74				

techniques. The results are analyzed using analysis of variance. The input parameters are optimized. The optimized values of output responses are obtained using grey relational analysis (GRA). The wear test conducted on the fabricated product with input parameters load, sliding speed, and percentage of reinforcement. The wear rate of the tool observed before and after drilling to study the wear rate of the tool after machining the hybrid metal matrix composite, and it is compared with the wear rate of the tool after machining the metal matrix composites. Figure 1 explains the experimental set up from machining of hybrid metal matrix composites and measurement of output responses such as torque, thrust forces, ovality, surface roughness, and temperature, the analysis of output responses using six sigma

Table 10: Output responses of machining operation.

Ex no.	Speed (rpm)	Feed (mm/min)	Drill Dia (mm)	Torque (N-m)	Thrust force (N)	Surface roughness (μm)	Ovality (mm)	Temp (°C)
1	600	25	4	26.7	194	4.67	0.006	26
2	600	25	8	29.6	199	5.06	0.007	27
3	600	25	12	57.45	260	8.27	0.009	30
4	600	50	4	13.1	305	6.8	0.001	26
5	600	50	8	17.5	315.2	7	0.002	32
6	600	50	12	23.6	410	8	0.003	40
7	600	75	4	15.5	437	11	0.0005	49
8	600	75	8	26.5	458	10.86	0.002	72
9	600	75	12	67.43	488	13.04	0.002	72
10	1230	25	4	32	100.1	4.8	0.003	27
11	1230	25	8	43.26	170.3	5.4	0.004	30
12	1230	25	12	96.8	230	7.08	0.005	32
13	1230	50	4	32	149.5	6.74	0.002	28
14	1230	50	8	39.23	184.1	7.8	0.002	31
15	1230	50	12	96.5	270	7.86	0.003	34
16	1230	75	4	12.75	245.6	7.56	0.002	28
17	1230	75	8	16.91	271	8.71	0.004	30
18	1230	75	12	25.36	340	11.5	0.006	32
19	1860	25	4	16.88	131	3.65	0.001	25
20	1860	25	8	22.6	300.9	4.06	0.003	26
21	1860	25	12	48.1	310	6.37	0.005	35
22	1860	50	4	13	147.7	5.87	0.001	30
23	1860	50	8	36.06	231	6	0.001	38
24	1860	50	12	56.04	320	8.46	0.001	45
25	1860	75	4	14.6	170.9	7.5	0.004	29
26	1860	75	8	24.11	257.1	7.52	0.006	41
27	1860	75	12	88.6	340	9.54	0.007	43

techniques, and optimization of input parameters using grey relational analysis.

2. Analyze the Output Response Using Six Sigma Techniques and Response Surface Methodology

2.1. Analysis of Torque. Torque is measured using dynamometer connected to the vertical machining center. Torque is measured using a graphical form. The measured torque is analyzed using six sigma technique. Figures 2(a) and 2(b) show the main effect plot for means and signal-to-noise ratio.

In mean plot, the input parameter speed increased to a maximum value, and then, it reduced and in signal-to-noise ratio, the minimum speed is obtained at 1230 rpm, and then, it increased. The feed rate is maximum at 25 mm/min for mean plot whereas for signal-to-noise ratio, the feed rate is minimum at 25 mm/min. In mean plot, the drill diameter is maximum at 12 mm drill diameter, and in signal-to-noise plot, the minimum value is obtained at 12 mm drill diameter. Figures 2(c) and 2(d) explain the interaction plot of means and signal-to-noise ratio in which each parameter is plotted in two different ways for better understanding. Figures 2(e) and 2(f) show the normal probability plot. Residuals are closer to diagonal line which represents ideal normal distribution, and the data is normally distributed. Figure 2(g) represents the histogram of torque with respect to frequency. The data values are in same interval size; at 10 Nm, the frequency level is 4; for 20 Nm, the graph shows the highest frequency of 7. The addition of all frequency values gives the normal frequency value of 27. Figure 2(h) shows empirical cumulative distribution function (CDF). CDF is the integral of probability distribution function. Figures 2(f), 2(i), and 2(j) explained the variation of output response torque with respect to speed, feed, and drill diameter. The R-square value in the table represent the percentage of data closer to the regression line.

The response of torque is listed in Table 1. This table displays the three levels of input parameters, and it influenced output response. Torque values are influenced by drill diameter with rank 1, and it is followed by speed with rank 2 and finally feed rate with rank 3. Analysis of variance (ANOVA) is the group of statistical models, and it is used to analyze the difference between the groups and among the groups. Mean

Table 11: S/N ratio and normalization values of output responses.

S/N ratio					Normalization				
Torque (N-m)	Thrust force (N)	Surface roughness (μm)	Ovality (mm)	Temp (°C)	Torque (N-m)	Thrust force (N)	Surface roughness (μm)	Ovality (mm)	Temp (°C)
-14.22	-31.44	0.927	58.7	-13.98	0.3651	0.8510	0.1938	0.2138	0.0000
-15.11	-31.66	0.23	57.41	-14.31	0.4157	0.8551	0.2568	0.2265	0.0359
-20.87	-33.98	-4.04	55.23	-18.75	0.7428	0.8982	0.6429	0.2481	0.5196
-8.03	-36.46	-2.34	74.31	-13.98	0.0136	0.9444	0.4892	0.0595	0.0000
-10.55	-35.65	-2.59	68.29	-15.79	0.1567	0.9293	0.5118	0.1190	0.1972
-13.14	-37.94	-3.75	64.77	-17.73	0.3038	0.9719	0.6166	0.1538	0.4085
-9.46	-38.49	-6.5	80.33	-19.49	0.0948	0.9821	0.8653	0.0000	0.6002
-14.15	-38.9	-6.4	-20.8414	-22.83	0.3612	0.9898	0.8562	1.0000	0.9641
-22.26	-39.45	-7.99	-20.3908	-22.83	0.8217	1.0000	1.0000	0.9956	0.9641
-15.7	-25.69	0.69	64.77	-14.31	0.4492	0.7440	0.2152	0.1538	0.0359
-18.4	-10.45	0.33	62.27	-15.23	0.6025	0.4605	0.2477	0.1785	0.1362
-25.4	-32.92	-2.69	60.33	-15.79	1.0000	0.8785	0.5208	0.1977	0.1972
-15.78	-29.18	-2.26	68.29	-14.63	0.4537	0.8089	0.4819	0.1190	0.0708
-17.56	-30.98	-3.53	68.29	-15.51	0.5548	0.8424	0.5967	0.1190	0.1667
-25.37	14.3	-3.59	64.77	-16.31	0.9983	0.0000	0.6022	0.1538	0.2538
-7.79	-33.49	-3.26	68.29	-14.63	0.0000	0.8891	0.5723	0.1190	0.0708
-10.24	-34.35	-4.49	62.27	-15.23	0.1391	0.9051	0.6835	0.1785	0.1362
-13.77	-36.32	-6.9	58.75	-15.79	0.3396	0.9418	0.9014	0.2133	0.1972
-10.233	-28	3.07	74.31	-13.65	0.1387	0.7870	0.0000	0.0595	-0.0359
-12.77	-35.25	2.14	64.77	-13.98	0.2828	0.9219	0.0841	0.1538	0.0000
-19.33	-35.51	-1.77	60.33	-16.56	0.6553	0.9267	0.4376	0.1977	0.2810
-7.96	-29.07	-1.06	74.31	-15.23	0.0097	0.8069	0.3734	0.0595	0.1362
-16.83	-32.96	-1.25	74.31	-17.28	0.5133	0.8793	0.3906	0.0595	0.3595
-20.71	-35.79	-4.23	74.31	-18.75	0.7337	0.9319	0.6600	0.0595	0.5196
-8.97	-30.34	-3.18	42.27	-14.93	0.0670	0.8305	0.5651	0.3762	0.1035
-13.33	-33.89	-3.21	58.75	-17.94	0.3146	0.8966	0.5678	0.2133	0.4314
-24.64	-36.32	-5.28	57.41	-18.35	0.9568	0.9418	0.7550	0.2265	0.4760

square value in ANOVA is obtained by dividing sum of squares (SS) by degrees of freedom (DF). The F value is the ratio between the variance of group means and mean of within group variances. The P value is used to determine the smallest level of significance by avoiding the null hypothesis (Table 2).

2.2. Analysis of Thrust Force. Thrust force on a surface is normal and perpendicular to the normal reaction on the surface. Thrust force is measured using dynamometer in a vertical machining center in a graphical form. It is revealed that the thrust force is minimum at the entry and exit of tool, and it is maximum during the drilling process [25]. Figures 3(a) and 3(b) show the mean and signal-to-noise ratio, and they are opposite to each other. Main effect plot for means shows the peak point at 600 rpm, 75 mm/min of feed rate, and at 12 mm drill diameter and the corresponding speed, feed rate, and drill diameter are least in signal-to-noise ratio. Figures 3(c) and 3(d) explained the interaction plot for both means and signal-to-noise ratio, and it explained that each factor is plotted in two different ways. Figure 3(e) shows the histogram plot of thrust force in equal intervals with respect to frequency. Figure 3(f) shows the empirical CDF of thrust force in terms of percentage. Figures 3(e)–3(g) explain the 3D surface plot of thrust force with respect to the combination of two input parameters. Thrust force increased to the largest with feed compared to the speed. Similarly, thrust force increased to the largest with drill diameter compared to speed. The percentage of thrust force closer to the regression line is about 96.78%. Tables 3 and 4 describe response table and ANOVA table for thrust force.

2.3. Analysis of Surface Roughness. Surface roughness of the drilled hole is measured using a profilometer by moving the probe of the profilometer along the drilled surface, and the corresponding values are obtained in the graphical form. Figures 4(a) and 4(b) represent main effect plot for means and signal-to-noise ratio, and the minimum surface roughness is obtained at 1860 rpm, 25 mm/min of feed rate, and 4 mm drill diameter for means, and the values are entirely conflicted with the signal-to-noise ratio. Figures 4(c) and 4(d) represent the interaction plot for means and signal-to-noise ratio, and it displayed the two different models in which each parameter is plotted. Figure 4(e) shows the

Table 12: Grey relational coefficient and grey relational code values of output responses.

Grey relational coefficient (GRC)					GRG
Torque (N-m)	Thrust force (N)	Surface roughness (μm)	Ovality (mm)	Temp (°C)	
0.4406	0.7704	0.3828	0.3887	0.3333	0.4632
0.4611	0.7753	0.4022	0.3926	0.3415	0.4745
0.6603	0.8309	0.5833	0.3994	0.5100	0.5968
0.3364	0.8999	0.4946	0.3471	0.3333	0.4823
0.3722	0.8761	0.5059	0.3621	0.3838	0.5000
0.4180	0.9468	0.5660	0.3714	0.4581	0.5521
0.3558	0.9655	0.7877	0.3333	0.5557	0.5996
0.4390	0.9799	0.7767	1.0000	0.9329	0.8257
0.7371	1.0000	1.0000	0.9912	0.9329	0.9323
0.4758	0.6614	0.3892	0.3714	0.3415	0.4479
0.5571	0.4810	0.3993	0.3784	0.3666	0.4365
1.0000	0.8045	0.5106	0.3839	0.3838	0.6166
0.4779	0.7235	0.4911	0.3621	0.3498	0.4809
0.5290	0.7604	0.5536	0.3621	0.3750	0.5160
0.9966	0.3333	0.5569	0.3714	0.4012	0.5319
0.3333	0.8185	0.5390	0.3621	0.3498	0.4805
0.3674	0.8405	0.6124	0.3784	0.3666	0.5131
0.4309	0.8957	0.8353	0.3886	0.3838	0.5869
0.3673	0.7012	0.3333	0.3471	0.3255	0.4149
0.4108	0.8648	0.3531	0.3714	0.3333	0.4667
0.5919	0.8721	0.4706	0.3839	0.4102	0.5458
0.3355	0.7214	0.4438	0.3471	0.3666	0.4429
0.5068	0.8055	0.4507	0.3471	0.4384	0.5097
0.6525	0.8801	0.5953	0.3471	0.5100	0.5970
0.3489	0.7468	0.5348	0.4449	0.3580	0.4867
0.4218	0.8286	0.5364	0.3886	0.4679	0.5286
0.9205	0.8957	0.6711	0.3926	0.4883	0.6737

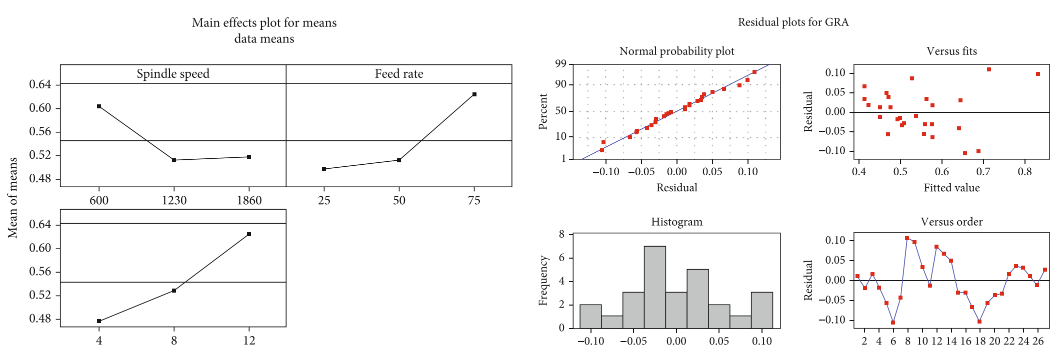

(a) Main effect plot for means (GRG)

(b) Residuals plots for GRG

Figure 7: Detail plot of GRG.

histogram of surface plot, and it is used to derive normal residual plot as well as probability plot. Figure 4(f) displays the empirical cumulative distribution, and it represents the integral of probability distribution function. Figure 4(g) represents 3D surface plot in which surface roughness increased with the increased combination of feed and drill diameter. Figure 4(h) proved the closeness of predicted value with the actual values. 92.4% of surface roughness values are accumulated closer to regression line, and it is represented as the R-square value. Response table of surface roughness indicates the influence of each input parameters on the output response surface roughness. The three levels of input parameters are listed in Table 5. Feed rate is influenced more on surface roughness with rank 1, and then drill diameter

Table 13: Response table for grey relational grade (GRG).

Level	Spindle speed (rpm)	Feed rate (mm/min)	Drill diameter (mm)
1	0.6029	0.4959	0.4776
2	0.5122	0.5125	0.5301
3	0.5184	0.6252	0.6259
Delta	0.0907	0.1294	0.1482
Rank	3	2	1

Table 14: ANOVA table for GRG.

Source	DF	SEQ SS	ADJ SS	ADJ MS	*F*	*P*
Regression	9	0.266755	0.266755	0.029639	6.19	0.001
Linear	3	0.206308	0.206308	0.029639	6.19	0.001
Spindle speed	1	0.032132	0.032132	0.032132	6.71	0.019
Feed rate	1	0.075312	0.075312	0.075312	15.73	0.001
Drill diameter	1	0.098864	0.098864	0.098864	20.65	0.001
Residual error	17	0.081385	0.081385	0.004787		
Total	26	0.34814				

Table 15: Confirmation test to optimize the input parameters.

Drilling parameters	Initial design	Optimal parameters	
		Prediction	Experiment
	A1B3C3	A3B2C1	A3B2C1
Torque	67.43		13
Thrust force	488		147.7
Surface roughness	13.04		5.87
Ovality	0.002		0.001
Temperature	72		30
Grey relational grade	0.9323	0.5445	0.4429

placed the next rank followed by spindle speed. ANOVA table for surface roughness is shown in Table 6. It explained the sum of square and mean square of linear form of input parameters, square values of input parameters, and interaction values of input parameters and their corresponding *P* and *F* values.

2.4. Analysis of Ovality. Ovality is the dimensional change along its diameter, horizontally and vertically. Ovality is measured by the profile projector. The drilled hole is projected on the screen with cross wires; then, the readings are noted using micrometers in the projector. Ovality occurred due to the heat generated during drilling operation. Figures 5(a) and 5(b) show the main effects plot for means and signal-to-noise ratio, and it describes variation of input parameters speed, feed rate, and drill diameter. Figures 5(c) and 5(d) display the interaction plot for means and signal-to-noise ratio. Figure 5(e) elaborates the histogram plot of ovality in terms of frequency in equal intervals; this histogram graph is related to normal probability distribution plot. Figure 5(f) represents empirical CDF of ovality in percentage. Figures 5(g)–5(i) describe the 3D surface plot of ovality in the combination of speed, feed rate, and drill diameter. This graph explains there is a drastic increase in ovality with the increasing range of feed rate and drill diameter. Figure 5(j) shows the graph plotted between the actual value and predicted value, and the actual values are accumulated along the regression line. 89.95% of data gradually gathered along the regression line and it is denoted as *R* square.

Table 7 shows the response table for means (ovality) listed the three different levels of input parameters. The influence of feed rate on ovality is more since it is assigned to rank 1 followed by drill diameter which holds the second rank and with lower influence on ovality is spindle speed and it is assigned with the rank 3. ANOVA (Table 8) shows the analysis of variance such as speed, feed rate, and the drill diameter.

2.5. Analysis of Temperature. The temperature for each hole is determined by pointing the infrared temperature indicator in a position while the tool performs the drilling operation, and it indicates the specific temperature. Figures 6(a) and 6(b) represent the main effects plot for means as well as signal-to-noise ratio. In means plot, the maximum value is obtained at 600 rpm and minimum value is obtained at 1230 rpm, and it reverses in the signal-to-noise ratio. Figures 6(c) and 6(d) show the interaction plot for means and signal-to-noise ratio, and it explains the input parameters are plotted in two different ways. Figures 6(e)–6(g) are related to each other; the normalization plot is obtained from histogram of temperature in terms of frequency. The empirical CDF is obtained from the integral of probability distribution function. This normal residual plot shows the closest distribution of temperature data towards the regression line. Figures 6(h)–6(j) explain that, as the diameter increase the temperature increased, similarly when the feed rate increases the temperature increased and the value of temperature decreased as the speed increased. *R*-square value represent the accumulation of temperature data along the regression line of about 71.86%. Response table for temperature represents that the influence of feed rate is more on temperature which is assigned to be rank 1; then, the percentage of influence of speed on temperature plays the second role and then the spindle speed (Table 9 (a)). Table 9(b) displays the analysis of variance table for temperature which listed the sum of squares; mean squares; F value and P value for linear form of input parameters of input parameters speed, feed rate, and drill diameter; square form of speed, feed rate, and drill diameters; and the interaction between the input parameters.

3. Optimize the Input Parameters Using Grey Relational Analysis (GRA) Techniques

GRA is one of the measurements in a grey system which briefs the correlation between the main factor and all other factors. It is an effective tool for multiresponse optimization. GRA used to evaluate and describe the relation of two or more things to the others when their direction of development is either varied or similar. Optimization is an essential action to select the effective input parameters for the responses obtained from machining. In this work, grey relational optimization is used. In this case, the output responses are listed in Table 10. For the corresponding input parameters, namely, spindle speed, feed rate, and drill diameter, the responses recorded are torque, thrust force, surface roughness, ovality and temperature, and smaller the better response is preferred for all the output responses.

3.1. Calculation of Signal-to-Noise Ratio and Normalization. The data obtained from the experiments are converted into signal-to-noise (S/N) ratio, and normalization values by the formula are listed in Table 11. The value obtained is negative since smaller the better concept is chosen, and the analysis is done to reduce the output response. Normalized the output responses as Z_{ij} using the formula: $Z_{ij} = \max(y_{ij}) - y_{ij}/\max(y_{ij}) - \min(y_{ij})$, where i is the number of experiments and j is the number of responses.

3.2. Calculation of Grey Relational Code. Grey relational coefficient (GRC) for the responses are calculated using the formula $G_{ij} = (\Delta \min + \varepsilon\Delta \max)/(\Delta_{ij} + \varepsilon\Delta \max)$, where Δ min is the minimum value, Δ max is the maximum value, and ε ranges from 0 to 1; then, the corresponding data are listed in Table 12. Grey relation grade (GRG) is calculated using the formula $\text{GRG} = (1/M). \sum G_{ij}$ and M is the number of responses The optimized input parameters are obtained from the response table for GRC. The highest value is termed as rank 1, and its corresponding parameters are optimized inputs. Spindle speed of 600 rpm in level 1, 75 mm/min of feed rate in level 3, and 12 mm of diameter in level 3 are the optimized input values. Figure 7(a) shows the main effect plot of grey relational grade (GRG). The maximum value of speed is obtained at 600 rpm, 75 mm/min, and 12 mm of drill diameter. A1B3C3 is the initial design where A represents spindle speed, B feed rate, and C drill diameter. Figure 7(b) displays the normal probability plot, fits, and histogram; all the four graphs are related to each other. In normal plot, the accumulation of data towards the regression lines indicate the less deviation, and this normal probability plot is derived from the histogram of residuals or GRG in terms of frequency. Response table for grey relational grade is displayed in Table 13. The input process parameters is listed in three levels in which the optimized value is chosen to be maximum. According to the spindle speed, level 3 is maximum compared to level 2 and 1. Feed rate and drill diameter level 3 are the maximum value compared to the other levels, so the predicted value is termed as A3B2C1, which is the predicted design, where A represents spindle speed, B represents feed rate, and C represents drill diameter. Table 14 is the analysis of variance which listed sequential sum of squares, mean sum of squares, F value, and P value. The optimal condition is set, and the selected experiments are carried out. The confirmation test is the final step to analyze the result obtained from the experiment. The average results obtained from the experiment is compared with the predicted average values. The optimal condition is set, and the selected experiments are carried out. The confirmation test is displayed in Table 15, and it shows the percentage is approximately equal.

4. Conclusion

Response surface methodology is used to generate the R -square value of the output responses which reveals the percentage of data accumulated along the regression line. Six sigma techniques are used to analyze the output responses using nominal probability plot, histogram plot, and main effect plot for means and noise-to-signal ratio while drilling hybrid metal matrix composites. The input parameter of feed rate and drill diameter greatly influenced the thrust force than the spindle speed.

4.1. The Data Are Analyzed Using Six Sigma and Response Surface Methodology

(a) Drill diameter and speed values greatly influenced the torque compared to spindle speed during drilling process

(b) Among the input parameters, the feed rate value is greatly influenced the thrust force and the corresponding R-square value is 96.78%

(c) The surface roughness is raising along with the feed rate, and it declines as the spindle speed increased and the corresponding R-square value is 92.4%

(d) In the output response, ovality is obtained using the optical projector and analyzed and the response is highly affected by feed rate and drill diameter. As the feed rate increases, the ovality increased and it decreased as the spindle speed increased and the accumulation of date along the regression line is 89.95%.

(e) The output response, temperature, is mainly dependent on federate and spindle speed compared to drill diameter, and the R-square value is 71.86%.

4.2. The Optimized Input Parameters Are Obtained Using Grey Relational Analysis. The optimized input parameters are obtained using grey coefficient grade. The level of optimized input parameters is A1B3C3. The corresponding optimized values of input parameters are spindle speed of 600 rpm ($A1$), feed rate value of 75 mm/min ($B3$), and drill diameter of 12 mm ($C3$), and the confirmation test reveals that the predicted and experimental values are approximately equal, and hence, the design is significant.

Data Availability

The data used for the study is used in the manuscript itself.

Conflicts of Interest

On behalf of all authors, the corresponding author states that there is no conflict of interest.

References

[1] J. A. Ghani, A. Choudhury, and H. H. Hassan, "Application of Taguchi method in the optimization of end milling parameters," *Journal of Materials Processing Technology*, vol. 145, no. 1, pp. 84–92, 2004.

[2] K. Giasin and S. Ayvar-Soberanis, "An investigation of burrs, chip formation, hole size, circularity and delamination during drilling operation of GLARE using ANOVA," *Composite Structures*, vol. 159, pp. 745–760, 2017.

[3] J. Fernandez-Perez, J. L. Cantero, J. Diaz-Alvarez, and M. H. Miguelez, "Influence of cutting parameters on tool wear and hole quality in composite aerospace components drilling," *Composite Structures*, vol. 178, pp. 157–161, 2017.

[4] E. Ekici, A. R. Motorcu, and G. Uzun, "An investigation of the effects of cutting parameters and graphite reinforcement on quality characteristics during the drilling of Al/10B_4C composites," *Measurement*, vol. 95, pp. 395–404, 2017.

[5] S. H. Tomadi, J. A. Ghani, C. H. Che Haron, H. Mas Ayu, and R. Daud, "Effect of cutting parameters on surface roughness in end milling of AlSi/AlN metal matrix composite," *Procedia Engineering*, vol. 184, pp. 58–69, 2017.

[6] M. Nataraj and K. Balasubramanian, "Parametric optimization of CNC turning process for hybrid metal matrix composite," *International Journal of manufacturing Technology*, vol. 93, no. 1-4, pp. 215–224, 2017.

[7] S. K. Lalmuan, S. Das, M. Chandrasekaran, and S. K. Tamang, "Machining investigation on hybrid metal matrix composites-a review," *Materials Today Proceedings*, vol. 4, no. 8, pp. 8167–8175, 2017.

[8] D. E. Patil and V. A. Kamble, "Optimization of drilling parameters for material removal rate, hole accuracy and surface roughness by using grey relational analysis," *International Journal for Innovative Research in Science & Technology*, vol. 2, pp. 2349–6010, 2016.

[9] D. Priyadarshi and R. K. Sharma, "Effect of type and percentage of reinforcement for optimization of the cutting force in turning of aluminium matrix nanocomposites using response surface methodologies," *Journal of Mechanical Science and Technology*, vol. 30, no. 3, pp. 1095–1101, 2016.

[10] E. Baburaj, K. M. Sundaram, and P. Senthil, "Effect of high speed turning operation on surface roughness of hybrid metal matrix (Al-SiCp-fly ash) composite," *Journal of Mechanical Science and Technology*, vol. 30, no. 1, pp. 89–95, 2016.

[11] U. A. Dabade and M. R. Jadhav, "Experimental study of surface integrity of Al/SiC particulate metal-matrix composites in hot machining," *Procedia CIRP*, vol. 41, pp. 914–919, 2016.

[12] G. Pichayyapillai, P. Seenikannan, K. Raja, and K. Chandrasekaran, "Al6061 hybrid metal matrix composite reinforced with alumina and molybdenum disulphide," *Advances in Materials Science and Engineering*, vol. 2016, 9 pages, 2016.

[13] P. C. Mishra, D. K. Das, M. Ukamanal, B. C. Routara, and A. K. Sahoo, "Multi-response optimization of process parameters using Taguchi method and grey relational analysis during turning AA 7075/SiC composite in dry and spray cooling environments," *International Journal of Industrial Engineering Computations*, vol. 6, no. 4, pp. 445–456, 2015.

[14] S. Karabulut, "Optimization of surface roughness and cutting force during AA7039/Al2O3 metal matrix composites milling using neural networks and Taguchi method," *Measurement*, vol. 66, pp. 139–149, 2015.

[15] C. Shoba, N. Ramanaiah, and D. N. Rao, "Optimizing the machining parameters for minimum surface roughness in turning Al/6% SiC/6%RHA hybrid composites," *Science*, vol. 10, pp. 220–229, 2015.

[16] K. Palanikumar and A. Muniaraj, "Experimental investigation and analysis of thrust force in drilling cast hybrid metal matrix (Al-15%SiC-4%graphite) composites," *Measurement*, vol. 53, pp. 240–250, 2014.

[17] G. Chaudhary, M. Kumar, S. Verma, and A. Srivastav, "Optimization of drilling parameters of hybrid metal matrix composites using response surface methodology," *Procedia Materials Science*, vol. 6, pp. 229–237, 2014.

[18] G. M. Umesh Gowda, H. V. Ravindra, H. R. Gurupavan, G. Ugrasen, and G. V. Naveen Prakash, "Optimization of process parameters in drilling Al- Si_3N_4 metal matrix composites material using Taguchi technique," *Procedia Materials Science*, vol. 5, pp. 2207–2214, 2014.

[19] K. Venkatesan, R. Ramanujam, J. Joel et al., "Study of cutting force and surface roughness in machining of Al alloy hybrid composite and optimized using response surface methodology," *Procedia Engineering*, vol. 97, pp. 677–686, 2014.

[20] P. Jayaraman and K. L. Mahesh, "Multi-response optimization of machining parameters of turning AA6063 T6 aluminium alloy using grey relational analysis in Taguchi method," *Procedia Engineering*, vol. 97, pp. 197–204, 2014.

[21] C. R. Prakash Rao and M. S. Bhagyashekar, "Effect of machining parameters on the surface roughness while turning particulate composites," *Procedia Engineering*, vol. 97, pp. 421–431, 2014.

[22] P. Ghabezi and M. Khoran, "Optimisation of drilling parameters in composite sandwich structures (PVC core)," *Indian Journal of Science Research*, vol. 2, pp. 173–179, 2014.

[23] P. Suresh, K. Marimuthu, S. Ranganathan, and T. Rajmohan, "Optimization of machining parameters in turning of Al-Sic-Gr hybrid metal matrix composites using grey-fuzzy algorithm," *Transactions of Nonferrous Metals Society of China*, vol. 24, no. 9, pp. 2805–2814, 2014.

[24] R. Ramanujam, N. Muthukrishnan, and R. Raju, "Optimization of cutting parameters for turning Al-SiC (10p) MMC using ANOVA and grey relational analysis," *International Journal of Precision Engineering and Manufacturing*, vol. 12, no. 4, pp. 651–656, 2011.

[25] M. Sangeetha and S. Prakash, "Experimental investigation of process parameters in drilling LM25 composites coated with multi wall carbon nano tubes using sonication process," *Achieves of Metallurgy and Materials*, vol. 62, no. 3, pp. 1761–1770, 2017.